Article

Cation distributions and anion disorder in $BaNbMO_{6}$ (M = Mo, W) materials: Implications for oxide ion conductivity

Josie E. Auckett, Katherine L. Milton, and Ivana Radosavljevic Evans

Chem. Mater., **Just Accepted Manuscript** • DOI: 10.1021/acs.chemmater.8b05179 • Publication Date (Web): 08 Feb 2019

Cation distributions and anion disorder in $Ba_3NbMO_{8.5}$ (*M* = Mo, W) materials: Implications for oxide ion conductivity

Josie E. Auckett,* Katherine L. Milton and Ivana Radosavljevic Evans*

Department of Chemistry, Durham University, South Road, Durham, DH1 3LE, United Kingdom

ABSTRACT: Competitive oxide ion conductivity has been identified recently in members of the $Ba_3Nb_{1-y}(Mo_{1-x}W_x)_{1+y}O_{8.5+½y}$ ($0 \le x \le 1$, $-0.3 \le y \le 0.2$) series, which adopt a disordered rhombohedral "hybrid" structure combining features of the 9R perovskite and palmierite structures. We report the first growth of $Ba_3NbMoO_{8.5}$ and $Ba_3NbWO_{8.5}$ single crystals from molten phases and their characterisation using single-crystal x-ray diffraction data between 120 and 473 K. Structure refinements reveal a previously unreported splitting of the central Nb/*M* cation site, rationalised by bonding considerations, which imposes limitations on the material stoichiometry and possible arrangements of cations within the face-sharing polyhedral stacks. Analysis of atomic displacement parameters and bond valence energy landscapes (BVELs) gives new insight into the probable low-energy pathways for oxide ion diffusion in the hybrid structure, indicating that they are three-dimensional and involve all crystallographically distinct oxygen sites. Evidence for considerable static disorder of the oxide ions at temperatures below the onset of significant conductivity is also discussed.

The urgent drive to replace fossil fuel-based energy sources with cleaner alternatives has prompted intensive research into the optimisation of new and diverse energy-generation technologies. For example, safe generation of electricity from the oxidation of hydrogen fuel is achieved in solid oxide fuel cells (SOFCs), but commercialisation of these devices has been hindered by a lack of solid cathode and electrolyte materials that conduct oxide ions efficiently at economically viable "moderate" operating temperatures (673–923 K).[1]

Oxide ion conductivity has been explored widely in systems such as defect fluorite-type oxides, perovskites and their derivatives, apatites and rare-earth molybdates (LAMOX materials),[2] but its discovery and characterisation in lesser-known oxide families is also of great interest. One recent high-profile example is the discovery of oxide ion conductivity in the $Ba_3Nb_{1-y}(Mo_{1-x}W_x)_{1+y}O_{8.5+½y}$ ($0 \le x \le 1$, $-0.3 \le y \le 0.2$) series which adopts a structure described as a hybrid of the 9R perovskite ($A_3B_3O_9$) and palmierite ($A_3B_2O_8$) types.[3, 4] The rhombohedral hybrid structure contains triple stacks of face-shared, *B*-centred polyhedra similar to those present in 9R perovskite, but the three possible *B* sites in each hybrid stack accommodate an average of only two *B* cations disordered over the three sites. This contrasts with the palmierite structure whose two *B* cations are located in the terminating polyhedra only so that the central *B* position is always vacant (Figure 1). Additionally, the terminating polyhedra in the hybrid stacks may adopt either 9R-like octahedral coordination or palmierite-like tetrahedral coordination depending on which of the crystallographic O2 or O3 sites is locally occupied. The average hybrid unit cell with $R\bar{3}m$ symmetry is therefore characterised by considerable crystallographic disorder.

Competitive oxide ion conductivity of 2.2×10^{-3} S cm^{-1} in $Ba_3NbMoO_{8.5}$ at 873 K was first reported by Fop *et al.*, who also described excellent thermal stability of the material under various atmospheres.[4, 5] More recently, members of the $Ba_3NbMo_{1-x}W_xO_{8.5}$,[6, 7] $Ba_3Nb_{1-y}Mo_{1+y}O_{8.5+½y}$[8] and $Ba_3Nb_{1-y}W_{1+y}O_{8.5+½y}$[9] series, including the end-member $Ba_3NbWO_{8.5}$,[10] have all been identified as generally isostructural with the disordered average structure of $Ba_3NbMoO_{8.5}$ and characterised as oxide ion conductors. In many of these studies, a correlation has been noted between the ratio of $M1O_4$ tetrahedral and $M1O_6$ octahedral units (determined by refinement against synchrotron or neutron powder diffraction data) and the magnitude of ionic conductivity as a function of temperature and composition. However, the relationship between M1 coordination and oxygen content in the average structure has not been fully explored, and questions remain concerning the possible mechanisms of oxygen diffusion in these materials. We were therefore motivated to explore the structural chemistry of $Ba_3NbMO_{8.5}$ phases in sufficiently fine detail – not attainable from the powder diffraction data published to date – to provide new insight into the relationships between the structure and properties of the hybrid structure family. Herein we present the first single crystal growth of $Ba_3NbMO_{8.5}$ phases, detailed structural analysis based on single-crystal x-ray diffraction, and a discussion of implications for identifying oxide ion migration pathways in this new and promising class of fast ion conductors.

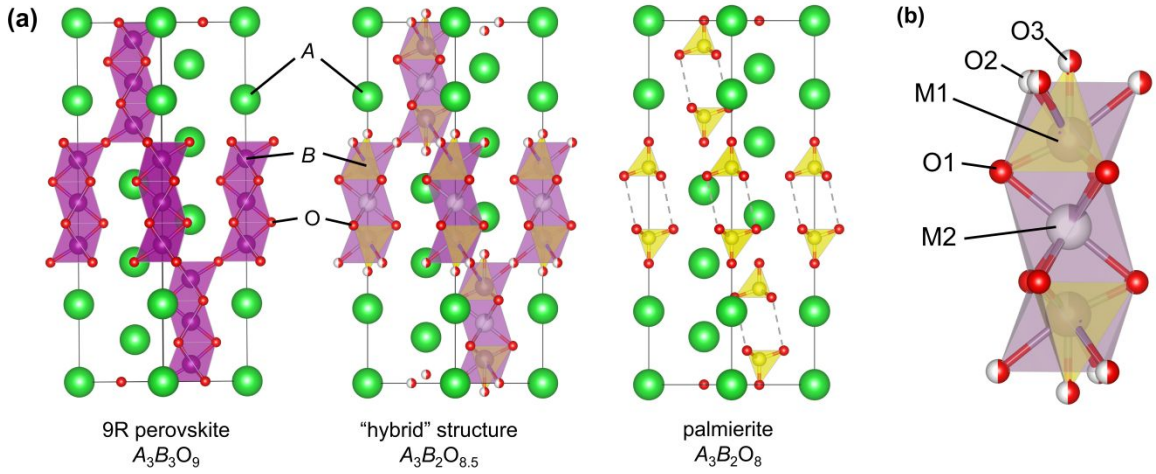

Figure 1. (a) Comparison of the "hybrid" structure with 9R perovskite and palmierite. (b) Detail of the hybrid structure showing the face-sharing polyhedral stack and crystallographic site labels for the *B* and O atoms. Atomic structure and density map diagrams throughout this paper were drawn using VESTA[11]. Split shading shows a partially occupied site.

Polycrystalline samples of $Ba_3NbMoO_{8.5}$ and $Ba_3NbWO_{8.5}$, synthesised in line with procedures published elsewhere,[7] were formed into rods and recrystallised from the molten phase using an optical floating-zone (FZ) furnace. Full details of all synthesis and characterisation procedures may be found in the Supporting Information. The FZ-solidified rods of both samples were visibly polycrystalline and appeared to contain grains of different colours, suggesting partial decomposition of the phases during the FZ growth experiment. Nevertheless, by gently crushing the rods it was possible to isolate optically transparent crystals up to ~10^{-3} mm^3 in volume, some of which exhibited the expected rhombohedral unit cell of the $Ba_3Nb\mathit{M}O_{8.5}$ hybrid structure. One such specimen of each composition was selected for laboratory single-crystal x-ray diffraction experiments at 120, 290 and 473 K.

Structure refinements were performed in Jana2006[12] using published structures of $Ba_3NbMoO_{8.5}$ and $Ba_3NbWO_{8.5}$[7] as starting models. Fractional occupancies of the mixed Nb/*M* sites were refined at 120 K only with constraints applied as discussed in the Supporting Information. A small three-fold splitting of the O3 site from the ideal 6*c* to an 18*h* position was applied, in accordance with previous studies,[9, 10] in order to account for local disorder. Unacceptably large agreement indices of *wR* ~ 19% were obtained using these models, with further inspection of the data and fit statistics revealing systematic over-calculation of the most intense reflections in all data sets. Furthermore, the fractional occupancy of the M2 site tended to approach zero when refined freely with an isotropic ADP, whereas allowing anisotropic displacement resulted in ellipsoids that were extremely elongated along the *c* axis (as also observed in the only previously published refinements for which the M1 and M2 ADPs were not made isotropic or constrained to be equal[10]). A Fourier difference map (F_{obs}–F_{calc}) calculated for $Ba_3NbWO_{8.5}$ clearly indicated unmatched electron density both above and below (with respect to the *c* axis) the nominal 3*b* Wyckoff position of the M2 site (Figure S1). Accordingly, this site was "split" onto a 6*c* position by translating it 0.01 lattice units along *c* and then refining its *z* parameter. Substantial improvements to the goodness of fit were achieved in all refinements after adopting this site splitting, and final agreement indices of 3–6% were obtained. Crystallographic parameters for both materials are summarised in Table S1, and full structural parameters are given in Tables S2 and S3. Refined fractional occupancies gave 11.9(3) and 20.5 (1) % occupation of the M2 site by *B* cations in $Ba_3NbMoO_{8.5}$ and $Ba_3NbWO_{8.5}$, respectively. We note that unresolvable ambiguities in the Nb:*M* ratio of the crystals as well as the distribution of *B* species between the M1 and M2 sites are not expected to alter the main crystallographic findings of this work (see Supporting Information).

Selected interatomic distances arising from the split-M2 site model refinements at 290 K are presented in Table 1. The refined M2 site parameters reveal a shift of nearly 0.6 Å away from the central 3*b* position, resulting in two mutually exclusive cation positions. Each possible $M2O_{16}$ octahedron is therefore highly distorted, containing three long (~2.5 Å) and three short (~1.8 Å) M2–O1 bonds. The $M1O_3O2_3$ octahedron, while more regular than $M2O_{16}$, is also strongly distorted (three ~2.2 Å and three ~1.6–1.7 Å bonds). Bond valence sums (BVSs)[13] calculated for the *B* cations at 290 K (Table 2) illustrate that these distorted octahedra provide more favourable bonding environments for the Nb^{5+} and M^{6+} ions than the 3*b* site at the centre of the $M2O_{16}$ octahedron, where they would be substantially underbonded. We also note that similar distortions are frequently observed in materials containing these cations in octahedral coordination[14-16] and discussed in terms of second-order Jahn-Teller effects.[17]

The proximity of each M2 site to its nearest M1 neighbour (~1.5 Å) indicates that simultaneous occupation of these cation positions would be highly unfavourable. Each polyhedral stack can therefore be occupied by a maximum of two cations, arranged in one

of the three possible configurations depicted in Figure 2. Because the chemical formula dictates an average of two cations per stack, no other configurations containing fewer occupied sites are possible if the stoichiometry is nominal. A further consequence is that the total number of *B* cations in the formula cannot exceed 2; this is in contrast to the 9R perovskite structure ($A_3B_3O_9$) which always contains three cations in the triple-octahedral stack and for which, to our knowledge, no significant splitting of the central site has ever been reported. This is understood by considering that all 9R-type oxides currently included in the International Crystal Structure Database (ICSD)[18] contain tetravalent *B* cations, which are likely to be more well-suited to the environment at the centre of the M2 octahedron than the high-oxidation state cations in the title compositions.

Table 1. Selected intersite distances from refinements against single-crystal x-ray diffraction data at 290 K.

	$Ba_3NbMoO_{8.5}$	$Ba_3NbWO_{8.5}$
M1–O1	1.827(3)	1.830(4)
M1–O2	2.2025(6)	2.1552(5)
M1–O3	1.71(2)	1.59(5)
M2–O1	1.797(4), 2.550(6)	1.780(4), 2.491(5)
M2–M1	1.493(7)	1.591(3)
M2′–M1	2.726(7)	2.744(3)
M2–M2′	1.234(9)	1.153(4)

Table 2. Bond valence sums (BVSs) calculated for *B* cations in the refined structures of $Ba_3NbMoO_{8.5}$ and $Ba_3NbWO_{8.5}$ at 290 K.

	$Ba_3NbMoO_{8.5}$		$Ba_3NbWO_{8.5}$	
	Nb^{5+}	Mo^{6+}	Nb^{5+}	W^{6+}
M1 (average)	5.34(3)	5.29(3)	5.74(10)	5.84(10)
M1 (octahed.)*	*5.16*	*5.10*	*5.31*	*5.40*
M1 (tetrahed.)*	*5.53*	*5.47*	*6.18*	*6.3*
M2 (split)	4.67(3)	4.62(3)	4.95(3)	5.03(3)
M2 (centred)*	*3.46*	*3.42*	*3.76*	*3.82*

BVSs were determined using standard bond valence coefficients defined in Jana2006[12] and a d_{max} cutoff of 5 Å. *Values in italics were calculated after manually editing relevant positional or occupancy parameters of the refined average structure models.

Recently, ambient and variable-temperature crystallographic investigations of phases in the $Ba_3Nb_{1-y}(Mo_{1-x}W_x)_{1+y}O_{8.5+½y}$ series have appeared to demonstrate that the ratio of M1-centred octahedra and tetrahedra (defined as the ratio of O2 and O3 occupancy), determined by Rietveld refinements against neutron or synchrotron x-ray powder diffraction data, correlates with ionic conductivity.[5-10] However, limitations of this model arising from both geometric and stoichiometric constraints remain unresolved. If the M1 cations are considered to adopt only octahedral or tetrahedral coordination, the corner-sharing of O2 sites between neighbouring polyhedral stacks effectively causes each octahedron to impose octahedral coordination on its three neighbours. If strictly enforced, this would result in the formation of infinite ordered layers of tetrahedra or octahedra and a consequent change in the unit cell symmetry and dimensions (as the existing unit cell contains an odd number of corner-shared polyhedral layers) or, if less strict, large slabs of correlated polyhedra with disordered boundaries. Local ordering of polyhedral configurations was proposed as an explanation for structure modulations observed by García-González *et al.*[3] in electron diffraction images of $Ba_3NbMoO_{8.5}$, but even the 3:2 local ordering scheme proposed in that work involved recurring pairs of octahedral and tetrahedral neighbours, and no crystallographic evidence for extended layers of like-ordered polyhedra has ever been presented. Furthermore, charge balance dictates that the terminating O2/O3 layers of each polyhedral stack in the structure must contain 1.25 oxygen atoms on average in order to maintain the overall composition of $O_{8.5}$ (6 O1 atoms forming the central M2 octahedron plus 1.25 O2/O3 at each end = 6 + 2 × 1.25 = 8.5). Each ideal M1 tetrahedron accounts for 1 oxygen atom (O3 × 1) and each octahedron accounts for 1.5 oxygen atoms (O2 × 3 × ½ due to corner sharing), such that the required 1.25 average is only achieved by a 50:50 ratio of octahedra and tetrahedra. Oxidation of the sample is unfeasible due to the maximised cation oxidation states, and the redox stability of $Ba_3NbMoO_{8.5}$ up to 600 C under actively reducing conditions has been established by thermogravimetric analysis.[4] Therefore it is only possible to redistribute the oxide ions and maintain charge balance by allowing the formation of intermediate (non-ideal) M1 coordination environments.

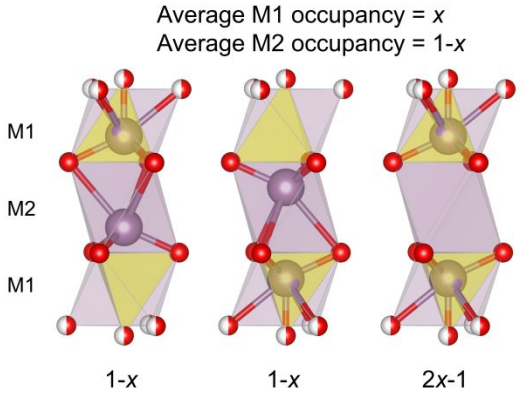

Figure 2. The three possible arrangements of two cations in the polyhedral stack in $Ba_3NbMO_{8.5}$. The O3 sites are depicted on a high-symmetry 6*c* site for simplicity.

Although fractional site occupancies for the light O atoms could not be refined reliably against our x-ray diffraction data, the refined ADPs yield clear insights into the disorder of oxide ions within the O2/O3 layers. The O2 ellipsoids in $Ba_3NbMoO_{8.5}$ are anomalously large

(equivalent $U_{iso} \approx 0.07$ Å^2) and are elongated between O3 sites (Figure 3). The size and shape of these ADPs even at room temperature, *i.e.* far below onset of significant conductivity, suggest primarily static disorder of oxide ions in the average model along those pathways. The refined structure of $Ba_3NbWO_{8.5}$ exhibits generally similar behaviour but with smaller ADPs for O2 and correspondingly larger ADPs for O3 in comparison to $Ba_3NbMoO_{8.5}$, pointing to a difference in the distribution of ions within the disordered networks of each material, though this difference cannot be characterised in further detail using x-ray diffraction alone. The splitting of the away from the three-fold rotation axis O3 site in both materials, adopted in all recent crystallographic studies and supported also by our refinements, is no doubt another symptom of this static disorder.

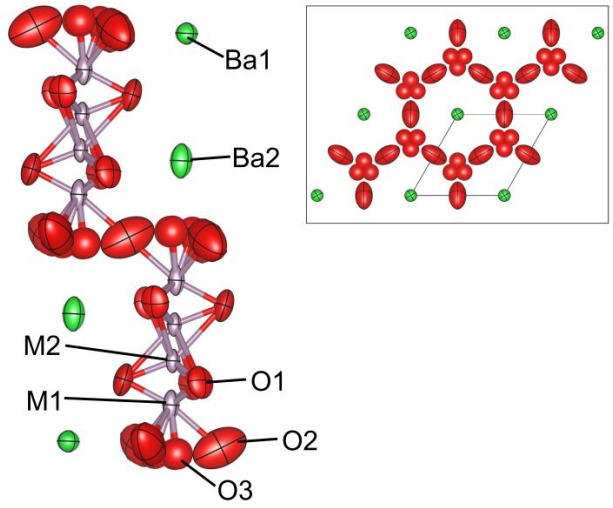

Figure 3. Portion of the disordered $Ba_3NbMoO_{8.5}$ structure refined against single-crystal x-ray diffraction data at 290 K. Displacement ellipsoids are shown at 95% probability. Inset: one O2/O3 layer viewed along the *c* axis.

As discussed above, the occurrence of neighbouring octahedral and tetrahedral units is assumed to be frequent and must be facilitated by local disruption to the ideal oxygen site configuration, because the distance between neighbouring nominal O2 and O3 sites (maximum ~2.2 Å) is too short to allow simultaneous occupation.[4, 5] The very large O2 ADPs illustrate a possible mechanism for producing intermediate M1 coordination environments, whereby an O2 atom in an octahedral unit (M1a) is displaced away from the occupied O3 site in a neighbouring "tetrahedral" unit (M1b), thus creating a distorted M1a-centred octahedron adjoining a M1b-centred 5-coordinate unit. It can be seen more generally that the necessary cooperative displacements of oxide ions from their average positions in the surrounding units would result in a variety of local arrangements whose exact geometry would depend on the bonding preference of the local M1 cation and the configurations of all three neighbouring polyhedra, leading to considerable positional disorder of oxide ions throughout the structure layers containing the O2 and O3 sites, as implied by our structure refinements.

The apparent variability the of M1 coordination sphere points to relatively shallow energy surfaces for O displacements, which is a desirable feature for reducing energy barriers to oxide ion diffusion in ionic conductors. In order to investigate possible pathways for oxide ion conduction, bond valence energy landscape (BVEL) maps were calculated for the refined structure of $Ba_3NbMoO_{8.5}$ at 290 K using the 3DBVSMAPPER program[19] with a grid spacing of 0.2 Å. Two variants of the structure, containing either all M1+vacancy+M1 or all M1+M2+vacancy polyhedral stacks, were constructed for comparison of the energy landscapes around these different local environments. Although based on straightforward calculations of empirical BVSs, BVEL analysis has been shown to reproduce well the known ionic conduction pathways in several well-characterised materials.[19] In the variant of $Ba_3NbMoO_{8.5}$ containing only M1 cations, low-energy pathways are identified connecting the O3 sites along spaces related to the elongated O2 ADPs, forming a hexagonal network of paths in the *a*-*b* plane (Figure 4a) as speculated in an earlier study.[5] Considerable connectivity parallel to the *c* axis is also observed *via* the O1 sites and vacant M2 polyhedra (Figure 4b). By contrast, occupation of the M2 site appears to reduce the facileness of oxide ion migration between the O1 layers and O2/O3 layers, especially in the vicinity of vacant M1 sites (Figure 4c). From these observations we can postulate that oxide ion conductivity in the hybrid structure is three-dimensional, is subject to considerable local variation depending on the occupation of nearby M1 and M2 sites, and may proceed along complex pathways involving all nominal O sites, rather than depending primarily on the quantity of tetrahedral units as suggested by earlier studies.[5-10] This situation is similar to $La_2Mo_2O_9$, where oxide ion conductivity was initially proposed to involve only a subset of the O-atom sites in the structure, based on the fractional occupancies and the ADPs derived from powder diffraction data.[20] Subsequent work based on single-crystal x-ray diffraction, neutron scattering and *ab initio* molecular dynamics simulations provided a more detailed picture of the structure and dynamics which suggested that all O sites were involved in the processes contributing to the oxide ion diffusion in the material, and relating the complex room temperature structure to high-temperature oxide ion conductivity.[21, 22]

In "variable-coordination-cation oxide ion conductors" it could be expected, based on the bonding preferences, for a molybdate to be a better performer than an isostructural tungstate. For example, small decrease in conductivity has been reported for $La_2Mo_2O_9$ on partial substitution of Mo^{6+} with W^{6+}. [23] More significant differences in oxide ion conductivity of isostructural vanadates and phosphates have been attributed to this effect. [24] In line with this, is also possible that the oxide ion migration pathways which rely on the variability of the M1 coordination, demonstrated in this work, are the reason for the differences in conductivity between $Ba_3MoNbO_{8.5}$ and $Ba_3WNbO_{8.5}$ (in favour of the molybdate) reported in the literature. [4-7]

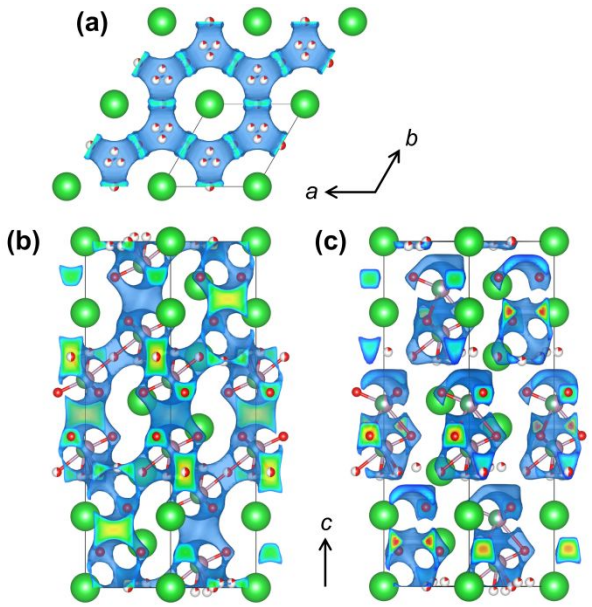

Figure 4. Bond valence energy landscape (BVEL) maps calculated for the refined structure of $Ba_3NbMoO_{8.5}$ (290 K) modified to contain only (a,b) M1+vacancy+M1 or (c) M1+M2+vacancy polyhedral stacks. Image (a) depicts a single layer of corner-shared M1 units viewed along the *c* axis. The isosurface level is –3.7 eV and the red limit of the colour scale, visible in the truncated cross sections, corresponds to –6 eV.

In conclusion, single crystals of the oxide-ion conductors $Ba_3NbMoO_{8.5}$ and $Ba_3NbWO_{8.5}$ exhibiting a hybrid rhombohedral perovskite structure have been grown and characterised for the first time. Diffraction data reveal a displacement of the M2 cation away from the centre of the triple polyhedral stack giving rise to a severely distorted central octahedral environment, which is adopted in order to optimise the bonding environment of the high-valence Nb^{5+} and M^{6+} cations. The splitting of this site allows limitations on the configuration of *B* cations in the polyhedral stacks to be deduced, and also precludes excess *B* cations in the composition of the hybrid structure. The correct modelling of these cation arrangements enables our structure refinements to capture for the first time the subtleties and the complexity of the true structure of these interesting materials. Experimental evidence and logical considerations together point to considerable positional disorder of the oxide ions within the structure layers containing the O2 and O3 sites, which would be necessary to allow variations between neighbouring M1 configurations while maintaining the overall oxygen stoichiometry of the sample. These findings yield a more nuanced description of the M1 coordination environment than the octahedral/tetrahedral dichotomy used previously, and suggest that the increase in refined O3 occupancy reported in various studies of $Ba_3Nb_{1-y}M_yO_{8.5}$ phases as a function of temperature[5, 6, 9] or composition[7, 8] may be better interpreted as a redistribution of the average ion positions (along the hexagonal conduction pathways) as their dynamic mobility increases, rather than a straightforward increase in the number of tetrahedral M1 units in the structure. Future work focusing on detailed characterisation of the oxide ion distributions at temperatures relevant to the onset of ionic conductivity (573–873 K), using single-crystal x-ray or neutron diffraction as well as local structure investigations such as total scattering analysis, is highly desirable for a fuller understanding of ionic conductivity mechanisms in the promising fast ion conductors with the $Ba_3NbMO_{8.5}$ hybrid structure.

ASSOCIATED CONTENT

Supporting Information. Details of all experimental methods; additional discussion of refined occupancy parameters; supplementary structure figures; full tables of refined parameters. This material is available free of charge via the Internet at http://pubs.acs.org.

AUTHOR INFORMATION

Corresponding Author

*I.R. Evans. Email: ivana.radosavljevic@durham.ac.uk
*J.E. Auckett. Email: josie.auckett@durham.ac.uk

ACKNOWLEDGMENT

The authors are grateful to Dr Dmitry Yufit for practical assistance with single-crystal x-ray diffraction experiments, Dr Leon Bowen for training and access to the GJ Russell Electron Microscopy Facility, and Mr Ian Chaplin for the preparation of specimens for SEM experiments. J.E.A. acknowledges the support of a Newton International Fellowship (NF170809) awarded by The Royal Society. I.R.E. acknowledges the Royal Society and the Leverhulme Trust for the award of a Senior Research Fellowship (SRF\R1\180040). This work was supported by the Engineering and Physical Sciences Research Council (EP/P020534/1).

REFERENCES

1. Gao, Z.; Mogni, L. V.; Miller, E. C.; Railsback, J. G.; Barnett, S. A., A perspective on low-temperature solid oxide fuel cells. *Energy Environ. Sci.* **2016,** 9, 1602-1644.
2. da Silva, F. S.; de Souza, T. M., Novel materials for solid oxide fuel cell technologies: A literature review. *International Journal of Hydrogen Energy* **2017,** 42, 26020-26036.
3. García-González, E.; Parras, M.; González-Calbet, J. M., Electron Microscopy Study of a New Cation Deficient Perovskite-like Oxide: $Ba_3MoNbO_{8.5}$. *Chemistry of Materials* **1998,** 10, 1576-1581.
4. Fop, S.; Skakle, J. M. S.; McLaughlin, A. C.; Connor, P. A.; Irvine, J. T. S.; Smith, R. I.; Wildman, E. J., Oxide Ion Conductivity in the Hexagonal Perovskite Derivative $Ba_3MoNbO_{8.5}$. *Journal of the American Chemical Society* **2016,** 138, 16764-16769.
5. Fop, S.; Wildman, E. J.; Irvine, J. T. S.; Connor, P. A.; Skakle, J. M. S.; Ritter, C.; McLaughlin, A. C., Investigation of the Relationship between the Structure and Conductivity of the Novel Oxide Ionic Conductor $Ba_3MoNbO_{8.5}$. *Chemistry of Materials* **2017,** 29, 4146-4152.

6. Bernasconi, A.; Tealdi, C.; Malavasi, L., High-Temperature Structural Evolution in the $Ba_3Mo_{(1-x)}W_xNbO_{8.5}$ System and Correlation with Ionic Transport Properties. *Inorganic Chemistry* **2018,** 57, 6746-6752.

7. Bernasconi, A.; Tealdi, C.; Mühlbauer, M.; Malavasi, L., Synthesis, crystal structure and ionic conductivity of the Ba3Mo1−xWxNbO8.5 solid solution. *Journal of Solid State Chemistry* **2018,** 258, 628-633.

8. Fop, S.; Wildman, E. J.; Skakle, J. M. S.; Ritter, C.; McLaughlin, A. C., Electrical and Structural Characterization of Ba3Mo1–xNb1+xO8.5–x/2: The Relationship between Mixed Coordination, Polyhedral Distortion and the Ionic Conductivity of Ba3MoNbO8.5. *Inorganic Chemistry* **2017,** 56, 10505-10512.

9. McCombie, K. S.; Wildman, E. J.; Ritter, C.; Smith, R. I.; Skakle, J. M. S.; McLaughlin, A. C., Relationship between the Crystal Structure and Electrical Properties of Oxide Ion Conducting Ba3W1.2Nb0.8O8.6. *Inorganic Chemistry* **2018,** 57, 11942-11947.

10. McCombie, K. S.; Wildman, E. J.; Fop, S.; Smith, R. I.; Skakle, J. M. S.; McLaughlin, A. C., The crystal structure and electrical properties of the oxide ion conductor Ba3WNbO8.5. *Journal of Materials Chemistry A* **2018,** 6, 5290-5295.

11. Momma, K.; Izuma, F., VESTA: a three-dimensional visualization system for electronic and structural analysis. *J. Appl. Crystallogr.* **2008,** 41, 653-658.

12. Petříček, V.; Dušek, M.; Palatinus, L., Crystallographic Computing System JANA2006: General features. In *Zeitschrift für Kristallographie - Crystalline Materials*, 2014; Vol. 229, p 345.

13. Brown, I. D.; Altermatt, D., Bond-valence parameters obtained from a systematic analysis of the Inorganic Crystal Structure Database. *Acta Crystallographica Section B* **1985,** 41, 244-247.

14. Vanderah, T. A.; Collins, T. R.; Wong-Ng, W.; Roth, R. S.; Farber, L., Phase equilibria and crystal chemistry in the BaO–Al_2O_3–Nb_2O_5 and BaO–Nb_2O_5 systems. *Journal of Alloys and Compounds* **2002,** 346, 116-128.

15. Miiller, W.; Auckett, J.; Avdeev, M.; Ling, C. D., Coexistence of spin glass and antiferromagnetic orders in $Ba_3Fe_{2.15}W_{0.85}O_{8.72}$. *Journal of Physics: Condensed Matter* **2012,** 24, 206004.

16. Menezes, L. A. D.; Atencio, D.; Andrade, M. B.; Downs, R. T.; Chaves, M.; Romano, A. W.; Scholz, R.; Persiano, A. I. C., Pauloabibite, trigonal $NaNbO_3$, isostructural with ilmenite, from the Jacupiranga carbonatite, Cajati, Sao Paulo, Brazil. *American Mineralogist* **2015,** 100, 442-446.

17. Kunz, M.; Brown, I. D., Out-of-Center Distortions around Octahedrally Coordinated d^0 Transition Metals. *Journal of Solid State Chemistry* **1995,** 115, 395-406.

18. Bergerhoff, G.; Brown, I. D., Inorganic crystal structure database. In *Crystallography Databases*, Allen, F. H.; Bergerhoff, G.; Sievers, R., Eds. International Union of Crystallography: Chester, 1987; pp 77-95.

19. Sale, M.; Avdeev, M., 3DBVSMAPPER: a program for automatically generating bond-valence sum landscapes. *Journal of Applied Crystallography* **2012,** 45, 1054-1056.

20. Goutenoire, F.; Isnard, O.; Suard, E.; Bohnke, O.; Laligant, Y.; Retoux, R.; Lacorre, P., Structural and transport characteristics of the LAMOX family of fast oxide-ion conductors, based on lanthanum molybdenum oxide $La_2Mo_2O_9$. *Journal of Materials Chemistry* **2001,** 11, 119-124.

21. Evans, I. R.; Howard, J. A. K.; Evans, J. S. O., The crystal structure of α-$La_2Mo_2O_9$ and the structural origin of the oxide ion migration pathway. *Chemistry of Materials* **2005,** 17, 4074-4077.

22. Peet, J. R.; Fuller, C. A.; Frick, B.; Zbiri, M.; Piovano, A.; Johnson, M. R.; Evans, I. R., Direct Observation of Oxide Ion Dynamics in $La_2Mo_2O_9$ on the Nanosecond Timescale. *Chemistry of Materials* **2017,** 29, 3020-3028.

23. Vega-Castillo, J. E.; Ravella, U. K.; Corbel, G.; Lacorre, P.; Caneiro, A., Thermodynamic stability of $La_2Mo_{2-y}W_yO_9$, $La_2Mo_{2-y}W_yO_{8.96+0.02y}$ and $La_7Mo_{7(2-y)/2}W_{7y/2}O_{30}$ (y=0, 0.5 and 1.0). *Dalton Transactions* **2014,** 43, 2661-2669.

24. Dunstan, M. T.; Halat, D. M.; Tate, M. L.; Evans, I. R.; Grey, C. P., Variable-temperature Multinuclear Solid-state NMR Study of Oxide Ion Dynamics in Fluorite-type Bismuth Vanadate and Phosphate Solid Electrolytes. *Chemistry of Materials,* **2019**, just accepted DOI: 10.1021/acs.chemmater.8b05143

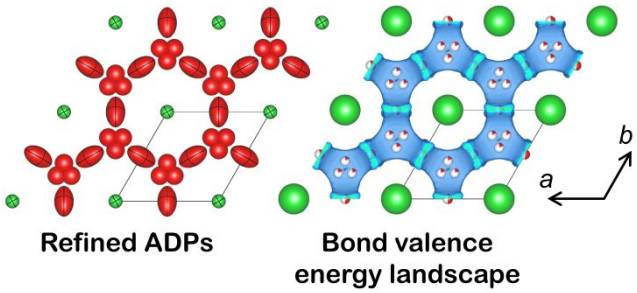
b
a
Refined ADPs
Bond valence
energy landscape